HHS Public Access

Author manuscript

Nat Med. Author manuscript; available in PMC 2014 October 01.

Published in final edited form as:

Nat Med. 2014 April ; 20(4): 377–384. doi:10.1038/nm.3467.

Netrin-1 promotes adipose tissue macrophage accumulation and insulin resistance in obesity

Bhama Ramkhelawon[1], **Elizabeth J Hennessy**[1], **Mickaël Ménager**[2], **Tathagat Dutta Ray**[1], **Frederick J Sheedy**[1], **Susan Hutchison**[1], **Amarylis Wanschel**[1], **Scott Oldebeken**[1], **Michele Geoffrion**[4], **Westley Spiro**[1], **George Miller**[3], **Ruth McPherson**[4], **Katey J Rayner**[4], and **Kathryn J Moore**[1]

[1]Department of Medicine, Marc and Ruti Bell Program for Vascular Biology and Disease, The Leon H. Charney Division of Cardiology, New York University School of Medicine, New York, NY, USA

[2]Molecular Pathogenesis Program, The Kimmel Center for Biology and Medicine of the Skirball Institute, New York University School of Medicine, New York, NY, USA

[3]Department of Surgery, New York University School of Medicine, New York, NY, USA

[4]University of Ottawa Heart Institute, Ottawa, Canada

Abstract

During obesity, macrophage accumulation in adipose tissue propagates the chronic inflammation and insulin resistance associated with type 2 diabetes. The factors that regulate the accrual of macrophages in adipose are not well understood. Here we show that the neuroimmune guidance cue netrin-1 is highly expressed in obese, but not lean adipose tissue of humans and mice, where it directs the retention of macrophages. Expression of netrin-1 is induced in macrophages by the saturated fatty acid palmitate, and acts via its receptor Unc5b to block macrophage migration. In a mouse model of diet-induced obesity, we show that adipose tissue macrophages exhibit reduced migratory capacity, which can be restored by blocking netrin-1. Furthermore, hematopoietic deletion of *Ntn1* facilitates adipose tissue macrophage emigration, reduces inflammation, and improves insulin sensitivity. Collectively, these findings identify netrin-1 as a macrophage retention signal in adipose tissue during obesity, which promotes chronic inflammation and insulin resistance.

Obesity and its co-morbidities, type 2 diabetes and cardiovascular disease, continue to increase and are major threats to global health. Studies in mice and humans have shown that

[5]Corresponding Author: Dr. Kathryn J Moore, Telephone: +1-212-2639498, Kathryn.Moore@nyumc.edu.

AUTHOR CONTRIBUTION

B.R., K.J.R, and K.J.M. conceived of the study; B.R. performed the *in vivo* studies, data analyses, and assisted in the preparation of the manuscript; E.J.H., W.S. and S.B. assisted with mouse studies; F.J.S. performed ELISA assays; M.M. assisted with flow cytometry studies, S.O. performed RT-PCR; G.M. and R.M. collected human samples; K.J.R. and M.G. performed serum netrin-1 ELISA; T.D.R performed western blots, A.W. performed migration assays; K.J.M. designed, analyzed and interpreted the studies and wrote the manuscript.

expansion of adipose tissue mass is closely associated with the recruitment of cells of the myeloid and lymphoid lineage[1–7], which gives rise to a state of chronic inflammation. The accumulation of adipose tissue macrophages (ATM) in obesity is striking, with ATMs comprising up to 40% of visceral white adipose tissue (VAT)[5]. These cells secrete pro-inflammatory molecules, including tumor necrosis factor alpha (TNFα),[8] interleukin-1 beta (IL-1β)[9,10], and CCL2[11], that contribute to the local and systemic inflammation that potentiate insulin resistance. The selective inhibition or genetic deficiency of factors that promote macrophage recruitment (eg. CCL2) or alter their inflammatory state (eg. IKKb) reduces adipose tissue inflammation and insulin resistance in obese mice[11,12]. In human studies, treatment of type 2 diabetics with the insulin-sensitizing thiazolidinediones showed a correlation between improved systemic insulin resistance and the reduction of ATMs and inflammatory factors[13,14]. These findings suggest that inflammation of the VAT compromises metabolic homeostasis.

Resident tissue macrophages are a heterogeneous population, and their phenotype and function reflect their local metabolic and immune microenvironment. Macrophages that populate lean adipose tissue are thought to be similar to alternatively-activated or M2 macrophages[15], which characteristically secrete anti-inflammatory cytokines (eg. IL-10) and promote tissue remodeling. With over-nutrition, increased numbers of classically activated or M1-like macrophages populate the VAT, where they secrete inflammatory factors that impair glucose homeostasis in this and other tissues[16]. Adipocyte-derived chemokines (eg. CCL2[17] and leukotriene B4[18]) and obesity-associated increases in lipolysis[19] are thought to provoke this influx of inflammatory monocyte-derived macrophages. However, studies have shown that the M1 and M2 macrophage phenotypes are not firmly entrenched, and interventions that alter key signaling molecules controlling alternative activation, such as the peroxisome proliferator activated receptor-γ, can regulate the dynamic balance of ATMs and insulin sensitivity[20].

Despite recent advances in our understanding of the immune cell types that accumulate in adipose tissue with obesity, the underlying mechanisms that promote their accrual and sustain chronic inflammation, are not well understood. We hypothesized that in addition to signals directing the recruitment of macrophages into adipose tissue, obesity would provoke signals that promote macrophage retention. Growing evidence supports roles for neuronal guidance molecules of the slit, semaphorin, ephrin and netrin families in regulating immune cell responses, including migration, adhesion and inflammatory status[21–24]. Indeed, a recent study showed increased expression of semaphorin 3E in the VAT of obese mice and humans, where it served to promote the recruitment and activation of macrophages[25]. Notably, such neuronal guidance cues act as both positive and negative regulators of cell migration.

Netrin-1 is a secreted laminin-related molecule that orients axonal growth cones through both chemoattractive and chemorepulsive signaling[22]. Netrin-1 achieves these opposing functions by engaging distinct receptors on its target cell: receptors of the DCC (Deleted in Colorectal Carcinomas) family, including DCC and neogenin, mediate chemoattraction to netrin-1, whereas members of the UNC5 family (UNC5A-D in mammals) and the adenosine A2 B receptor mediate chemorepulsion. Instructional roles for netrin-1 and its receptors

have been demonstrated in organogenesis[26,27], angiogenesis[28,29], tumorigenesis[30,31], and inflammation[32,33], suggesting that netrin-1 regulates cell migration in a broad context. Here we show that netrin-1 and its receptor Unc5b are highly expressed in obese but not lean adipose tissue of humans and mice, and investigate the contribution of this guidance cue to HFD-induced inflammation and insulin resistance.

RESULTS

Adipose expression of netrin-1 and Unc5b is regulated by obesity

To identify neuronal guidance cues regulated by obesity, we performed gene expression profiling of adipose tissue from C57BL/6J mice fed a chow or high-fat diet (60% Kcal) for 20 weeks. Using a custom expression array comprising a complete panel of netrin, semaphorin, slit and ephrin guidance cues and their receptors, we found that netrin-1 (*Ntn1*) mRNA was higher in VAT from HFD-fed obese mice than lean chow-fed mice (Fig. 1a and Supplementary Table 1). We confirmed that netrin-1 expression was higher in adipose tissue of HFD- compared to chow-fed mice by quantitative real-time PCR (qRT-PCR) (Fig. 1a) and western blotting (Fig. 1b), whereas, serum netrin-1 levels were similar in both groups (Supplementary Fig. 1a). Furthermore, mRNA and protein levels of the chemorepulsive netrin-1 and its receptor Unc5b were higher in adipose tissue of obese mice compared to lean mice, whereas expression of the chemoattractive receptors *Dcc* and *Neogenin* were similar in both groups (Fig. 1a,b). The high expression of *Ntn1* and *Unc5b* in obese adipose tissue was associated with high expression of the macrophage marker F4/80 (*Emr1*) and the pro-inflammatory cytokine genes *Il6* and *Tnfa* (Fig. 1a). In addition, the expression of other select neuroimmune guidance molecules was higher in adipose tissue of obese mice compared to lean mice such as *Sema3e* (Fig. 1a), which was recently reported to promote monocyte recruitment into adipose tissue during HFD-feeding[25].

To identify the cellular compartment expressing netrin-1 and Unc5b, we isolated mRNA from the adipocyte and stromal vascular fractions of VAT of chow- and HFD-fed mice and performed qRT-PCR analysis. *Ntn1* and *Unc5b* mRNA were higher in the stromal vascular, but not adipose fraction of HFD- compared to chow-fed mice (Fig. 1c). Consistent with this, immunofluorescence staining of VAT from HFD-fed mice showed netrin-1 and Unc5b reactivity in crown-like structures that co-localized with staining for the macrophage antigen F4/80 (Fig. 1d). Netrin-1 and Unc5b staining was not detected in VAT from lean mice (data not shown), indicating that this guidance cue-receptor pair is specifically expressed in macrophages that infiltrate obese VAT.

To investigate the translational relevance of our findings in mice, we measured the expression of netrin-1 and Unc5b in human adipose tissue from lean (BMI<25 kg/m^2) and obese (BMI>28 kg/m^2) individuals. *NTN1* and *UNC5H2 (*the homologue of *Unc5b)*, but not *DCC* mRNA were higher in adipose from obese compared to lean subjects, as was expression of the macrophage marker *CD68* and the inflammatory cytokine *TNFA. SEMA3E* was also higher in obese compared to lean subjects, whereas mRNA for other neuronal guidance cues with immunoregulatory functions, such as *SEMA3A,* were similarly expressed (Fig. 2a). Immunofluorescence staining showed netrin-1 reactivity in adipose tissue from obese, but not lean individuals, that co-localized with CD68-positive macrophages in crown-

like structures (Fig. 2b). Interestingly, netrin-1 serum concentrations were lower in obese (mean BMI 38.6 kg/m^2) than lean (mean BMI 18.2 kg/m^2) individuals (Supplementary Fig. 1b), suggesting that netrin-1 is selectively increased in ATM during obesity.

Palmitate regulates netrin-1 and Unc5b expression

We next sought to understand the mechanisms underlying ATM expression of netrin-1 and Unc5b during obesity. Free fatty acids (FFA) are substantially elevated by HFD and are important adipocyte-derived mediators of macrophage inflammatory responses[34,35]. We tested whether palmitate, a saturated fatty acid that is abundant during obesity, could induce expression of netrin-1 and Unc5b in bone marrow derived macrophages (BMDM). *Ntn1* and *Unc5b* mRNA was 5- and 3-fold higher, respectively, in BMDMs treated with palmitate conjugated to fatty acid-free bovine serum albumin (BSA) than BSA alone (Fig. 3a). Furthermore, palmitate, but not BSA, induced the activity of *Ntn1*- and *Unc5b*-promoter luciferase reporter genes in HEK293 cells, which was inhibited, in part, by pretreating cells with an inhibitor of NFkB, BAY 11-7085 (Fig. 3b,c). Moreover, palmitate, but not BSA, induced secretion of netrin-1 by BMDM as measured by ELISA, which was inhibited by BAY 11-7085 (Fig. 3d).

As a number of studies have demonstrated paracrine interactions between adipocytes and macrophages in the WAT during inflammation[34], we next investigated whether adipocyte inflammatory factors secreted during obesity could induce ATM expression of netrin-1. We harvested conditioned medium from 3T3L1 adipocytes treated with palmitate or BSA, and used this to treat BMDM. Secreted factors from palmitate-, but not BSA-treated adipocytes induced *Ntn1* and *Unc5b* mRNA in BMDM (Fig. 3e). As previously reported[36,37], palmitate-treated adipocytes express high levels of *Tnfa* and *Il6* mRNA (Fig. 3f), and we showed that treating BMDMs with TNFα or IL-6, but not IL-4, increased *Ntn1* mRNA (Fig. 3g). To test the role of these cytokines, conditioned media from palmitate- and BSA-stimulated 3T3L1-adipocytes were incubated with TNFα and IL-6 blocking antibodies, either alone or in combination, and used to treat BMDM. Antibodies to TNFα or IL-6, but not control IgG, partially blocked the induction of *Ntn1* and *Unc5b* mRNA by conditioned medium from palmitate-stimulated adipocytes (Fig. 3h and Supplementary Fig. 2), supporting a role for adipocyte-derived TNFα and IL-6 in the induction of netrin-1 and Unc5b in neighboring macrophages.

Netrin-1 promotes defective ATM migration and accumulation

As netrin-1 has recently been reported to inhibit macrophage migration, we hypothesized that its secretion by ATMs may induce macrophage chemostasis and block the egress of these cells from the VAT. To test this, we isolated CD11b+F4/80+ ATM from mice fed chow or HFD for 16 weeks, and measured their migration to the chemokine CCL19, which has been implicated in the emigration of tissue macrophages to draining lymph nodes. Notably, ATMs isolated from obese mice exhibit lower migration to CCL19 than ATMs from lean mice (Fig. 4a), despite equivalent expression of the CCL19 receptor *Ccr7* (Fig. 4b). By contrast, blood monocytes isolated from lean and obese mice showed similar levels of chemotaxis to CCL2 (Supplementary Fig. 3a), consistent with reports that circulating monocytes from chow and HFD-fed mice exhibit comparable recruitment to adipose tissue

in vivo[38]. Notably, ATMs from lean mice treated with netrin-1 showed lower migration to CCL19 compared to untreated ATMs (Fig. 4c). Furthermore, incubating ATMs from obese mice with a blocking antibody to Unc5b increased their ability to migrate to CCL19 to lean ATM levels (Fig. 4d), consistent with a role for netrin-1 in inducing ATM chemostasis during obesity. Moreover, peritoneal macrophages treated with palmitate showed lower migration to CCL19 than BSA-treated macrophages (Fig. 4e), which was restored by the addition of a chimeric Unc5b-FC peptide that competitively inhibits netrin-1, but not by a control FC (Fig. 4f). Similar findings were observed when CCL2 was used as a chemoattractant (Supplementary Fig. 3b,c).

Based on these data, we postulated that ATM expression of netrin-1 during obesity may promote the accumulation of these cells in VAT, and foster chronic inflammation and metabolic dysfunction. To test this, we generated mice with and without netrin-1 in macrophages by reconstituting the bone marrow of C57BL/6 mice with fetal liver cells from e14 *Ntn1*$^{-/-}$ or *Ntn1*$^{+/+}$ (WT) pups, and fed the mice a chow or HFD for 20 weeks. HFD-fed *Ntn1*$^{-/-}$ → *C57BL/6 and WT* → *C57BL/6* mice gained more weight than their chow-fed counterparts, however no differences in food intake (Supplementary Fig. 4a), or body weight and fat content as measured by dual-energy X-ray absorptiometry (DEXA) (Fig. 4g,h) were observed between the two genotypes. Notably, *Ntn1*$^{-/-}$ → *C57BL/6* and *WT* → *C57BL/6* mice fed a chow diet accumulated similar numbers of ATMs, whereas HFD-fed *Ntn1*$^{-/-}$ → *C57BL/6* mice showed lower expression of *Emr1* (F4/80) mRNA (Fig. 4i) and fewer F4/80+ cells in crown-like structures (Fig. 4j) in the VAT compared to HFD-fed *WT* → *C57BL/6* mice. ATMs isolated from HFD-fed *Ntn1*$^{-/-}$ → *C57BL/6* mice also had lower mRNA for pro-inflammatory cytokines and markers of M1 macrophages (*Nos2*, *Tnfa*, *Il6*) and higher mRNA for markers of reparative M2 macrophages (*Cd206*, Pparg, *Il10*) compared with HFD-fed *WT* → *C57BL/6* mice (Fig. 5a). Thus, deletion of hematopoietic *Ntn1* reduces ATM accumulation and restores the balance of M1 and M2 macrophages in obese adipose tissue.

To test whether netrin-1 affects macrophage mobilization into and out of VAT, monocytes were labeled *in vivo* with fluorescent beads and tracked over time[39]. We measured macrophage recruitment and retention in *WT* → *C57BL/6* and *Ntn1*$^{-/-}$ → *C57BL/6* mice by comparing the number of bead-positive macrophages that accumulate in VAT 3 days after labeling (the time of peak recruitment of labeled cells to tissues[39]), and 11 days later to assess the number of labeled macrophages remaining. HFD-feeding induced 2.5-fold greater recruitment of labeled monocytes into VAT compared to chow-feeding in both *WT* → *C57BL/6* and *Ntn1*$^{-/-}$ → *C57BL/6* mice (Fig. 5b; day 3). The fluorescent beads carried in by these monocytes accumulated within F4/80-positive macrophages present in crown-like structures (Fig. 5c) to a similar extent in HFD-fed *WT* → *C57BL/6* and *Ntn1*$^{-/-}$ → *C57BL/6* mice after 3 days (Fig. 5b). However, the number of bead-labeled macrophages in VAT stayed constant in HFD-fed WT →C57BL6 mice at day 14 (Fig. 5b,c), whereas there were 50% fewer bead-labeled macrophages in VAT of *Ntn1*$^{-/-}$ → *C57BL/6* mice at this time point compared to day 3. As the reduction in bead-labeled macrophages in the *Ntn1*$^{-/-}$ → *C57BL/6* mice at day 14 is indicative of ATM emigration from the VAT, we isolated the draining lymph nodes from the mesentery and analyzed the number of bead-labeled cells in

this tissue. The mesenteric lymph nodes of HFD-fed Ntn1$^{-/-}$ →C57BL6 contained 40% more bead-labeled cells than WT →C57BL6 mice at day 14 (Fig. 5d, Supplementary Fig. 4b). Together, these data suggest that netrin-1 secreted by ATMs acts as a retention signal to promote ATM accumulation in the setting of obesity.

Netrin-1 promotes insulin resistance in vivo

The accumulation of macrophages within VAT has been shown to correlate with systemic inflammation and metabolic dysfunction, and consistent with this, we observed lower serum TNFα concentrations in HFD-fed *Ntn1*$^{-/-}$ → *C57BL/6* mice compared to *WT* → *C57BL/6* mice (Fig. 6a). Furthermore, glucose and insulin tolerance tests (GTT and ITT) revealed that HFD-fed *Ntn1*$^{-/-}$ → *C57BL/6* mice had improved glucose homeostasis and insulin responsiveness compared to *WT* → *C57BL/6* mice (Fig. 6b,c), as well as lower fasting blood glucose (Fig. 6d), insulin (Fig. 6e) and FFA concentrations (Fig. 6f). Moreover, whereas plasma adiponectin concentrations were lower in HFD-fed *WT* → *C57BL/6* mice compared to chow-fed mice, no difference was observed in HFD-fed *Ntn1*$^{-/-}$ → *C57BL/6* mice (Fig. 6g). Finally, as the metabolic effects of insulin are dependent on phospho-inositol 3-kinase (PI3K)-AKT signaling in target tissues, we measured the phosphorylation of AKT on Ser473 in adipose tissue, liver and muscle of HFD-fed mice. Consistent with the improved insulin sensitivity in *Ntn1*$^{-/-}$ → *C57BL/6* mice, there was 2–4-fold more phospho-AKT in adipose tissue, liver and muscle of these mice compared to *WT* → *C57BL/6* controls (Fig. 6h). Together, these data indicate that loss of netrin-1 expression in ATMs leads to improved maintenance of glucose homeostasis and insulin sensitivity during obesity.

DISCUSSION

There is a clear association between ATM accumulation and insulin resistance with HFD-feeding, yet the factors that sustain chronic inflammation in obesity are not well defined. Our results uncover a key role for the neuroimmune guidance cue netrin-1 and its receptor Unc5b in the retention of macrophages in the VAT during obesity. The expression of netrin-1 and Unc5b axis is higher in ATMs of obese mice and humans compared to lean controls, where it induces macrophage chemostasis. Treating macrophages with palmitate to induce netrin-1 secretion or exposing ATMs from lean mice to netrin-1 impairs their migration to CCL19, a chemokine that directs the emigration of inflammatory macrophages and DCs from tissues to the lymph nodes. Notably, ATM isolated from obese mice exhibit impaired migration to CCL19, which is restored by blocking the netrin-1 receptor Unc5b, implicating netrin-1 in inducing ATM chemostasis. Indeed, the selective deletion of hematopoietic netrin-1 in mice fed a HFD reduces ATM accumulation in VAT, local and systemic inflammation, and insulin resistance. Collectively, these findings suggest that local secretion of netrin-1 by ATM promotes their retention in VAT and the chronic inflammation that leads to metabolic dysfunction.

To understand how netrin-1 promotes ATM accumulation in obesity, we adapted a fluorescent bead monocyte labeling technique that has been used to monitor the migration of macrophages into and out of atherosclerotic plaques[39,40]. *In vivo* macrophage tracking demonstrated that HFD-feeding induces 3-fold more recruitment of labeled macrophages

into the VAT of both *WT* → *C57BL/6* and *Ntn1*$^{-/-}$ → *C57BL/6* mice compared to chow-fed mice of each genotype. Notably, similar numbers of bead-labeled ATM were detected in VAT of HFD-fed *WT* → *C57BL/6* after 3 and 14 days, indicating that ATMs recruited to adipose of obese WT mice accrue in the tissue. By contrast, *Ntn1*$^{-/-}$ → *C57BL/6* mice had 50% fewer bead-labeled ATM in VAT and a greater number of bead-labeled cells in the mesenteric lymph nodes at day 14 compared to day 3, suggesting that ATMs emigrate from the VAT in the absence of netrin-1. These data suggest that during obesity netrin-1 acts downstream of monocyte chemoattractant signals, such as CCL2, to promote the local retention of ATM in VAT. Indeed, targeted deletion of netrin-1 in hematopoietic cells induces a phenotype similar to that observed in *Ccr2*$^{-/-}$ mice[11]: protection from HFD diet-induced adipose inflammation, and improved systemic glucose homeostasis and insulin sensitivity.

Studies in humans and animal models have shown that caloric restriction, or a switch from a high-fat to a low-fat diet, reduces adipose inflammation[41–43]. The signals controlling resolution of inflammation in the adipose tissue remain poorly defined, but are likely to involve reduced recruitment, local macrophage death and efferocytosis, as well as egress of macrophages from the inflammatory site. In other tissues, including the intestine[44] and atherosclerotic plaques[40,45], the chemokine receptor CCR7 has been shown to promote the trafficking of macrophages to the lymph nodes. We show herein that ATM isolated from obese, but not lean mice, exhibit impaired migration to the CCR7 ligand CCL19, despite equivalent expression of CCR7. Notably, the responsiveness to CCL19 could be restored in obese ATM by inhibiting the Unc5b receptor, suggesting that netrin-1 is responsible for this chemostasis. Previous studies have shown that netrin-1 inhibits Rac-mediated re-organization of the actin cyctoskeleton and cell spreading, key steps required for cell migration[33]. Although the signaling pathways regulating netrin-1 expression in ATM of obese mice and humans *in vivo* will require further experimentation, previous studies have shown that increased FFA concentrations promote macrophage accumulation in the VAT[19]. Indeed, we demonstrate that palmitate directly induces *Ntn1* and *Unc5b* expression by macrophages, and also upregulates expression of TNFα and IL-6 by neighboring adipocytes, which can in turn induce macrophage *Ntn1* and *Unc5b* expression.

Collectively, our studies suggest a model in which netrin-1 secreted by ATM in the setting of obesity acts as a “stop” signal to promote the accrual of these immune cells in the VAT. Macrophages, as a percent of total cells in the VAT, expand from ≈10% in lean individuals to more than 50% in advanced obesity, yet, the underlying cause and functions of these ATMs remain poorly understood. A number of hypotheses regarding the triggers of ATM accumulation have been put forth, including an increase in adipocyte death in the expanding adipose tissue[46], the release of saturated FFA that activate inflammatory signaling pathways[47,48], and the need for macrophages to buffer the lipids released from obese adipocytes in order to protect tissues from potentially toxic lipid levels[49]. These signals, either alone or combined, promote the sustained accumulation of ATM and inflammatory molecules that impair the metabolic function of the VAT. We postulate that netrin-1 may be turned on as a signal to locally trap ATMs during obesity to help the VAT in the clearance

of apoptotic adipocytes and the buffering of increased lipids, however, its sustained expression leads to chronic inflammation and the failure to reestablish tissue homeostasis.

It is notable that netrin-1 is selectively upregulated in the VAT, but not serum, of obese mice and humans. In fact, we observed a modest, but significant reduction in circulating levels of netrin-1 in obese individuals compared to lean controls, and a similar trend in HFD-fed mice. Although the implications of these findings are unknown, recent studies suggest that netrin-1 in the circulation may inhibit inflammation by reducing leukocyte recruitment into tissues. Netrin-1 is expressed on vascular endothelium and gut epithelium where its expression is regulated to promote or inhibit leukocyte transmigration into tissues[32,50–52]. Reduced circulating levels of netrin-1 have been associated with neutrophil infiltration of the kidney during ischemia-reperfusion injury[53,54]. Furthermore, lentiviral-overexpression of netrin-1 on endothelial cells protects *Ldlr*$^{-/-}$ mice from atherosclerosis[55], presumably by reducing leukocyte recruitment into the artery wall. However, netrin-1 is also abundantly expressed by macrophage foam cells in atherosclerotic plaques, where its expression promotes the accumulation of macrophages and disease progression[33], consistent with our findings in obese VAT. Thus, therapeutic targeting of netrin-1 to reduce chronic inflammation in obesity and atherosclerosis will require macrophage-targeted delivery of netrin-1 or Unc5b inhibitors to avoid unwanted effects on netrin-1 at the endothelium or epithelium.

Current strategies aimed at targeting adipose inflammation have so far yielded variable results: Blocking TNFα signaling in obese individuals with T2D produced suboptimal outcomes[56], yet clinical trials of IL-1 inhibition appear more promising[57]. However, these therapies directed at blocking cytokines that result from chronic inflammation are likely to be less effective than treatments targeting the source of this problem, ie. the sustained accumulation of macrophages and other immune cells in VAT. Our work suggests that targeting local factors that promote the retention of macrophages, such as the netrin-1/Unc5b axis, may reverse the local and systemic mediators of inflammation that drive metabolic dysfunction.

METHODS

Mice

6–8 week old male C57BL/6J mice and 26 week old male C57BL/6J mice fed a HFD consisting of 60% Kcal from fat (D12492, Research diets) or a control chow diet for 20 weeks were purchased from Jackson Laboratories. All mice were maintained in a pathogen-free facility. For bone marrow transplantation studies, female and male *Ntn1*$^{+/-}$ mice (10 generations backcrossed onto C57BL/6 background) were mated to generate *Ntn1*$^{+/+}$ and *Ntn1*$^{-/-}$ donor mice. On day 14 of gestation, embryos were dissected free from the placenta and yolk sac, and single-cell suspensions of fetal liver cells were prepared by flushing through graded sizes of needles. A portion of the fetal tissue was used for genotyping by 5-bromo-4-chloro-3-indoyl-β-d-galactoside staining and PCR analysis. Fetal liver cells (2×10^6) were injected intravenously into 6–8 week old recipient C57BL/6 mice that were lethally irradiated (two exposures of 600 cGy) and mice were allowed to recover for 6 weeks. C57BL/6J mice were fed a standard chow or HFD consisting of 60% Kcal from fat

(D12492, Research diets) for 20 weeks. At the termination of the study, mice were anesthetized with Tribomoethanol (0.4mg/g i.p.) and ex-sanguinated by cardiac puncture. Experimental procedures were done in accordance with the USDA Animal Welfare Act and the PHS Policy for the Human Care and Use of Laboratory Animals and the New York University School of Medicine's Research Animal Care and Use.

Human subjects

Visceral adipose tissue (omental and mesenteric) was collected from patients who underwent laparotomy for neoplastic disease at a site remote from the collection of visceral adipose tissue. The lean patients had a body mass index (BMI) ≤25 kg/m^2. Obese patients had a BMI ≥28 kg/m^2. The NYU School of Medicine IRB approved tissue collection. Serum concentrations of netrin-1 were measured a second group of healthy age matched (mean 71±1.5 yr) lean (BMI=18.2±1.4 kg/m^2;n=20;6M/14F) and obese patients (BMI=38.6±2.4 kg/m^2;n=20;9M/11F) recruited under an IRB approved protocol at the University of Ottawa Heart Institute.

Real-time Quantitative RT-PCR Analysis

RNA (0.5–1 μg) was reverse transcribed using iScriptTM cDNA Synthesis Kit (Biorad) and RT-PCR analysis was conducted using kapa SYBR green Supermix (kappa syber) and a Mastercycler Realplex (Eppendorf) the primers used are listed in (Supplemental Table 2). Fold change in mRNA expression was calculated using the comparative cycle method (ΔΔCt).

Gene Expression Profiling

1 mg of adipose tissue from either lean or obese animals was homogenized in TRIzol reagent (Invitrogen) using the Bullet BlenderTM (New England Bio Group) and total RNA isolated as we described[33]. RNA quality was verified by pico chip (5067-1511; Agilent technologies). Adipose RNA (1 μg) was reverse transcribed and quantitative RT-PCR analysis of the 4 families of the axonal guidance molecules was performed using RT2 Custom Profiler PCR Arrays (Qiagen) according to manufacturer's protocol. Data analysis was performed using the manufacturer's integrated web-based software package of the PCR Array System using ΔΔCt based fold- change calculations.

Adipocyte and ATM purification

Fat pads of mice were excised and minced in HBSS. Tissue suspensions were centrifuged at 500 g for 5 minutes to remove erythrocytes and free leukocytes. Liberase (5401119001; Roche applied science) was added to 1 mg/ml and incubated at 37°C for 30 minutes with shaking. The cell suspension was filtered through a 100-μm filter and then spun at 300 g for 5 minutes to separate floating adipocytes from the SVF pellet. To ensure proper isolation, adipocyte fractions were examined by microscopy before and after plating on plastic to detect adherent cells. Samples were digested until adipocyte fractions were free of adherent cells by these 2 quality-control methods to ensure recovery of the majority of the SVF population. For cell culture, the adipocytes were resuspended in growth media for further experiments. Isolation of CD11b+ cells from SVF isolates was performed by magnetic

immunoaffinity isolation with anti-CD11b antibodies conjugated to magnetic beads (10 μl/10^7 cells, 120-000-300; MACS Miltenyi Biotec). Cells were isolated using positive selection columns prior to preparation of whole-cell lysates.

Cell culture

Primary bone marrow derived macrophage (BMDM) was prepared by flushing the bone marrow of the tibia and femur of 6–8 week old C57BL/6J mice. The cells were grown in DMEM supplemented with 15% L929-conditioned media, 10% FBS and 1% penicillin/streptomycin for 7 days. BMDM were stimulated 250 μM palmitate conjugated with BSA or BSA as a control for 24 hours, or TNFα (10 ng/ml, 410-MT-010; R&D systems), IL-6 (40 ng/ml, 406-ML-005; R&D systems) and IL-4 (10 ng/ml, 404-ML-010; R&D systems) for 24 h. In some assays, differentiated BMDM were treated with conditioned media from 3T3-L1 adipocytes differentiated as described[58] and treated with 250 μM palmitate conjugated with BSA or BSA for 24 hours. In certain experiments, anti-TNFα (0.4 μg/ml, AF-410-NA; R&D systems) or anti-IL-6 (0.025 μg/ml, MAB406; R&D systems) blocking antibody or the same concentrations of IgG control (Normal Goat IgG: AB-108-C, Rat IgG1: MAB005; R&D systems) was added to conditioned media. Peritoneal macrophages were isolated as described[33]. Mice were injected intraperitoneally with 1 ml of 3% (wt/vol) thioglycolate to elicit sterile peritonitis with macrophage numbers peaking on day 4. Cells were collected by lavage and used for migration assays.

Palmitate-BSA preparation

Sodium palmitate (P9767; Sigma Aldrich) was dissolved in sterile water in to make a 100 mM solution by alternating heating and vortexing until the palmitate was dissolved: this occurred once the solution reached 70°C. Immediately after the palmitate dissolved, it was conjugated to serum-free DMEM containing 5% NEFA-free BSA, creating a 5 mM palmitate solution as described[59]. The 5 mM palmitate solution was shaken at 140 rpm at 40°C for 1 h and was then immediately used to treat the cells. Serum-free DMEM containing 5% NEFA-free BSA was used as the vehicle control.

Promoter-Luciferase assays

HEK293T cells were transfected with human NTN1 or Unc5H2 promoter-luciferase reporter constructs (SwitchGear Genomics) using LipofectamineTM 2000 (11668-019, Invitrogen). After transfection, media was changed and cells were treated with palmitate or BSA for 24 hours, in the presence or absence of the NFkB inhibitor BAY 11-7082 (10 μmol/L, emd Millipore). Luciferase activity was measured using the DUAL-Glo Luciferase Assay system (E1910, Promega).

Analytical procedures

Blood glucose values were determined from whole venous blood using an automatic glucose monitor (Freestyle Lite). The fat content in the mice was analyzed by dual x-ray absorptiometry (DXA) scanning. The mice were anesthetized and placed in the prone position on the specimen tray to allow scanning of the entire body. For food intake measurements, *WT* → *WT* and *Ntn1*$^{-/-}$ → *WT* mice were fed a 60% Kcal fat diet (D12492,

Research diets). Male mice were housed individually and were given a defined amount of large intact food pellet every 2 days. Food weight was measured using a balance with a precision of 0.01 g (Ohaus coorporation) and cages were changed. Solid food intake was corrected for any visible spillage[60].

Glucose-and insulin-tolerance tests

Glucose-tolerance tests were performed as previously described[61]. After determination of fasted blood glucose levels, each animal received a glucose gavage of 1.5 g/kg body weight of glucose (25% Dglucose, G7528; Sigma). Blood glucose levels were determined after 15, 30, 60 and 120 min. Insulin-tolerance tests were carried on unfasted animals by injecting an i.p injection of 1.5 U/kg body weight of insulin (HumilinR 100U/ml). Blood glucose levels were detected after 15, 30, 60, 120 and 240 mins.

ELISA assays

Insulin (90080; crystal Chem Inc), adiponectin (ab108785; Abcam), FFA (SFA-1; Zen Bio), TNFa (88-7064-76; ebiosciences) and netrin-1 (E91827Mu; USCN life science Inc) levels were measured in the serum or cell supernatants using mouse standards according to manufacturer's guidelines. Netrin-1 in human serum was measured using a human-specific netrin-1 ELISA from USCN Life Science Inc (700176; mybiosource).

Labeling and tracking of blood monocytes

Circulating blood monocytes were labeled in *WT* → *WT* and *Ntn1*$^{-/-}$ → *WT* mice fed a HFD for 20 weeks by retro-orbital intravenous injection of 1 μm Fluoresbite green fluorescent plain microspheres (Polysciences) diluted 1:4 in sterile PBS as described[33,39]. Labeling efficiency was assessed 1d after injection of beads. One group of mice was harvested after 3 days for baseline measurements, as this time point has previously been shown to have optimal recruitment of labeled monocytes into tissues and clearance of the labeled monocytes from the blood. A second group of mice was harvested 14 days later to measure the number of labeled macrophages remaining in adipose. Adipose tissue and mesenteric lymph nodes were sectioned (5 μM) and the number of beads per section (x20, x4) was counted from 9 slides per mouse.

Immunohistochemistry

White adipose tissue was excised, fixed in formalin overnight, embedded in paraffin and sectioned. The immunofluorescence analysis of netrin-1 (1:200, AF1109; R&D systems), caveolin-1 (1:500, 610059; BD bioscience), Unc5b (1:200, ab54430; Abcam), F4/80 (1:500, MCA497GA; Abd serotec), CD68 (1:500, MCA1957; Abd serotec) was conducted after deparaffinization as described previously[61]. Secondary antibodies were then applied (Alexa Fluor-568, A11011; Alexa Fluor-488, A11006; 1:500 Invitrogen). Netrin-1 and Unc5b staining was amplified using the biotin conjugated antibodies (1:100, BA-2000 and BA-9500; Vector Laboratories) followed by streptavidin conjugated AMCA (1:200, Sa-5008; Vector Laboratories) staining. Sections were mounted and visualized using a Nikon Eclipse microscope.

Migration

The migration of macrophages to CCL19 (500 ng/ml, 440-M3-025, R&D Systems) or CCL-2 (100 ng/ml, 479-JE-010, R&D Systems) was assessed by the xCelligence Real-time Cell Invasion and Migration system (ACEA biosciences Inc) that monitored chemotaxis every 5 minutes for over 6 h. Peritoneal macrophages or BMDMs were pretreated with 250 μM Palmitate or BSA prior to migration. The SVF fraction was isolated from mice fed a chow (lean) or HFD (obese) for 14–16 weeks as described above and the cells were sorted on magnetic columns to select for CD11b+/F4/80+ (10 μl/10^7 cells, NC97677703, 130-099-440, Miltenyi Biotec). In certain experiments, recombinant netrin-1 (250 ng/ml, 1109-NI-025, R&D Systems), rat Unc5b-Fc (1 μg/ml, 1006-UN-050, R&D Systems) or control IgG (110-HG-100, R&D Systems) was added to assay. Total blood was collected from either lean or obese mice and the mononuclear cells were separated using Histopaque (10771, Sigma Aldrich) solution. After 2 PBS washes, the cells were counted and labelled using CD11b (10 μL/10^7 cells, NC97677703, Miltenyi Biotec) and Ly6G (10 μL/10^7 cells, 120003029, Miltenyi Biotec). CD11b+Ly6G- cells were separated using magnetic columbs (130042201, Miltenyi Biotec) and migrated to CCL-2.

Western-blot analysis

The WAT, liver and muscle tissues were homogenized in lysis buffer as previously described[61]. Western-blot analyses were carried out according to standard protocols with antibodies raised against netrin-1 (MAB1109; R&D Systems), Unc5b (AF1006; R&D Systems), AKT (1:1000, 9272; Cell Signaling,), phosphoAKT Ser 473 (1:1000, 9271; Cell Signaling), and α-tubulin (1:5,000, T6074; Sigma) were used as loading controls.

Statistical methods

The difference between two groups was analyzed by Student's t-test or for multiple comparisons, by one-way analysis of variance, followed by Newman-Keus multiple comparison test. P values of less than 0.05 were considered significant.

Supplementary Material

Refer to Web version on PubMed Central for supplementary material.

ACKOWLEDGMENTS

Support for this work came from the US National Institutes of Health (RC1HL100815 to K.J.M; T32HL098129 to E.J.H), the American Heart Association (13POST14490016 to B.R), and Canadian Institutes of Health Research (MOP-2390941 to R.M.)

REFERENCES

1. Feuerer M, et al. Lean, but not obese, fat is enriched for a unique population of regulatory T cells that affect metabolic parameters. Nature medicine. 2009; 15:930–939.
2. Kintscher U, et al. T-lymphocyte infiltration in visceral adipose tissue: a primary event in adipose tissue inflammation and the development of obesity-mediated insulin resistance. Arteriosclerosis, thrombosis, and vascular biology. 2008; 28:1304–1310.
3. Liu J, et al. Genetic deficiency and pharmacological stabilization of mast cells reduce diet-induced obesity and diabetes in mice. Nature medicine. 2009; 15:940–945.

4. Nishimura S, et al. CD8+ effector T cells contribute to macrophage recruitment and adipose tissue inflammation in obesity. Nature medicine. 2009; 15:914–920.
5. Weisberg SP, et al. Obesity is associated with macrophage accumulation in adipose tissue. The Journal of clinical investigation. 2003; 112:1796–1808. [PubMed: 14679176]
6. Wu H, et al. T-cell accumulation and regulated on activation, normal T cell expressed and secreted upregulation in adipose tissue in obesity. Circulation. 2007; 115:1029–1038. [PubMed: 17296858]
7. Xu H, et al. Chronic inflammation in fat plays a crucial role in the development of obesity-related insulin resistance. The Journal of clinical investigation. 2003; 112:1821–1830. [PubMed: 14679177]
8. Hotamisligil GS, Shargill NS, Spiegelman BM. Adipose expression of tumor necrosis factor-alpha: direct role in obesity-linked insulin resistance. Science. 1993; 259:87–91. [PubMed: 7678183]
9. Vandanmagsar B, et al. The NLRP3 inflammasome instigates obesity-induced inflammation and insulin resistance. Nature medicine. 2011; 17:179–188.
10. Wen H, et al. Fatty acid-induced NLRP3-ASC inflammasome activation interferes with insulin signaling. Nature immunology. 2011; 12:408–415. [PubMed: 21478880]
11. Weisberg SP, et al. CCR2 modulates inflammatory and metabolic effects of high-fat feeding. The Journal of clinical investigation. 2006; 116:115–124. [PubMed: 16341265]
12. Arkan MC, et al. IKK-beta links inflammation to obesity-induced insulin resistance. Nature medicine. 2005; 11:191–198.
13. Koppaka S, et al. Reduced Adipose Tissue Macrophage Content Is Associated With Improved Insulin Sensitivity in Thiazolidinedione-Treated Diabetic Humans. Diabetes. 2013
14. Di Gregorio GB, et al. Expression of CD68 and macrophage chemoattractant protein-1 genes in human adipose and muscle tissues: association with cytokine expression, insulin resistance, and reduction by pioglitazone. Diabetes. 2005; 54:2305–2313. [PubMed: 16046295]
15. Lumeng CN, Bodzin JL, Saltiel AR. Obesity induces a phenotypic switch in adipose tissue macrophage polarization. The Journal of clinical investigation. 2007; 117:175–184. [PubMed: 17200717]
16. Lumeng CN, Deyoung SM, Bodzin JL, Saltiel AR. Increased inflammatory properties of adipose tissue macrophages recruited during diet-induced obesity. Diabetes. 2007; 56:16–23. [PubMed: 17192460]
17. Takahashi K, et al. Adiposity elevates plasma MCP-1 levels leading to the increased CD11b-positive monocytes in mice. The Journal of biological chemistry. 2003; 278:46654–46660. [PubMed: 13129912]
18. Chakrabarti SK, et al. Evidence for activation of inflammatory lipoxygenase pathways in visceral adipose tissue of obese Zucker rats. American journal of physiology. Endocrinology and metabolism. 2011; 300:E175–E187. [PubMed: 20978234]
19. Kosteli A, et al. Weight loss and lipolysis promote a dynamic immune response in murine adipose tissue. The Journal of clinical investigation. 2010; 120:3466–3479. [PubMed: 20877011]
20. Odegaard JI, et al. Macrophage-specific PPARgamma controls alternative activation and improves insulin resistance. Nature. 2007; 447:1116–1120. [PubMed: 17515919]
21. Suzuki K, Kumanogoh A, Kikutani H. Semaphorins and their receptors in immune cell interactions. Nature immunology. 2008; 9:17–23. [PubMed: 18087252]
22. Cirulli V, Yebra M. Netrins: beyond the brain. Nat Rev Mol Cell Biol. 2007; 8:296–306. [PubMed: 17356579]
23. Wu JY, et al. The neuronal repellent Slit inhibits leukocyte chemotaxis induced by chemotactic factors. Nature. 2001; 410:948–952. [PubMed: 11309622]
24. Takamatsu H, Kumanogoh A. Diverse roles for semaphorin-plexin signaling in the immune system. Trends in immunology. 2012; 33:127–135. [PubMed: 22325954]
25. Shimizu I, et al. Semaphorin3E-induced inflammation contributes to insulin resistance in dietary obesity. Cell Metab. 2013; 18:491–504. [PubMed: 24093674]
26. Srinivasan K, Strickland P, Valdes A, Shin GC, Hinck L. Netrin-1/neogenin interaction stabilizes multipotent progenitor cap cells during mammary gland morphogenesis. Dev Cell. 2003; 4:371–382. [PubMed: 12636918]

27. Salminen M, Meyer BI, Bober E, Gruss P. Netrin 1 is required for semicircular canal formation in the mouse inner ear. Development. 2000; 127:13–22. [PubMed: 10654596]
28. Nguyen A, Cai H. Netrin-1 induces angiogenesis via a DCC-dependent ERK1/2-eNOS feed-forward mechanism. Proc Natl Acad Sci U S A. 2006; 103:6530–6535. [PubMed: 16611730]
29. Wilson BD, et al. Netrins promote developmental and therapeutic angiogenesis. Science. 2006; 313:640–644. [PubMed: 16809490]
30. Arakawa H. Netrin-1 and its receptors in tumorigenesis. Nat Rev Cancer. 2004; 4:978–987. [PubMed: 15573119]
31. Fitamant J, et al. Netrin-1 expression confers a selective advantage for tumor cell survival in metastatic breast cancer. Proc Natl Acad Sci U S A. 2008; 105:4850–4855. [PubMed: 18353983]
32. Rosenberger P, et al. Hypoxia-inducible factor-dependent induction of netrin-1 dampens inflammation caused by hypoxia. Nature immunology. 2009; 10:195–202. [PubMed: 19122655]
33. van Gils JM, et al. The neuroimmune guidance cue netrin-1 promotes atherosclerosis by inhibiting the emigration of macrophages from plaques. Nature immunology. 2012; 13:136–143. [PubMed: 22231519]
34. Suganami T, Nishida J, Ogawa Y. A paracrine loop between adipocytes and macrophages aggravates inflammatory changes: role of free fatty acids and tumor necrosis factor alpha. Arteriosclerosis, thrombosis, and vascular biology. 2005; 25:2062–2068.
35. Boden G. Interaction between free fatty acids and glucose metabolism. Current opinion in clinical nutrition and metabolic care. 2002; 5:545–549. [PubMed: 12172479]
36. Uysal KT, Wiesbrock SM, Marino MW, Hotamisligil GS. Protection from obesity-induced insulin resistance in mice lacking TNF-alpha function. Nature. 1997; 389:610–614. [PubMed: 9335502]
37. Sabio G, et al. A stress signaling pathway in adipose tissue regulates hepatic insulin resistance. Science. 2008; 322:1539–1543. [PubMed: 19056984]
38. Oh DY, Morinaga H, Talukdar S, Bae EJ, Olefsky JM. Increased macrophage migration into adipose tissue in obese mice. Diabetes. 2012; 61:346–354. [PubMed: 22190646]
39. Tacke F, et al. Monocyte subsets differentially employ CCR2, CCR5, and CX3CR1 to accumulate within atherosclerotic plaques. The Journal of clinical investigation. 2007; 117:185–194. [PubMed: 17200718]
40. Feig JE, et al. LXR promotes the maximal egress of monocyte-derived cells from mouse aortic plaques during atherosclerosis regression. The Journal of clinical investigation. 2010; 120:4415–4424. [PubMed: 21041949]
41. Kovacikova M, et al. Dietary intervention-induced weight loss decreases macrophage content in adipose tissue of obese women. International journal of obesity. 2011; 35:91–98. [PubMed: 20531347]
42. Wang Q, et al. Differential effect of weight loss with low-fat diet or high-fat diet restriction on inflammation in the liver and adipose tissue of mice with diet-induced obesity. Atherosclerosis. 2011; 219:100–108. [PubMed: 21824616]
43. Jung DY, et al. Short-term weight loss attenuates local tissue inflammation and improves insulin sensitivity without affecting adipose inflammation in obese mice. American journal of physiology. Endocrinology and metabolism. 2013; 304:E964–E976. [PubMed: 23482446]
44. Diehl GE, et al. Microbiota restricts trafficking of bacteria to mesenteric lymph nodes by CX(3)CR1(hi) cells. Nature. 2013; 494:116–120. [PubMed: 23334413]
45. Trogan E, et al. Gene expression changes in foam cells and the role of chemokine receptor CCR7 during atherosclerosis regression in ApoE-deficient mice. Proc Natl Acad Sci U S A. 2006; 103:3781–3786. [PubMed: 16537455]
46. Cinti S, et al. Adipocyte death defines macrophage localization and function in adipose tissue of obese mice and humans. Journal of lipid research. 2005; 46:2347–2355. [PubMed: 16150820]
47. Shi H, et al. TLR4 links innate immunity and fatty acid-induced insulin resistance. The Journal of clinical investigation. 2006; 116:3015–3025. [PubMed: 17053832]
48. Suganami T, et al. Role of the Toll-like receptor 4/NF-kappaB pathway in saturated fatty acid-induced inflammatory changes in the interaction between adipocytes and macrophages. Arteriosclerosis, thrombosis, and vascular biology. 2007; 27:84–91.

49. Xu X, et al. Obesity activates a program of lysosomal-dependent lipid metabolismin adipose tissue macrophages independently of classic activation. Cell Metab. 2013; 18:816–830. [PubMed: 24315368]
50. Wang W, Reeves WB, Pays L, Mehlen P, Ramesh G. Netrin-1 overexpression protects kidney from ischemia reperfusion injury by suppressing apoptosis. Am J Pathol. 2009; 175:1010–1018. [PubMed: 19700747]
51. Mirakaj V, et al. Netrin-1 dampens pulmonary inflammation during acute lung injury. Am J Respir Crit Care Med. 2010; 181:815–824. [PubMed: 20075388]
52. Ly NP, et al. Netrin-1 inhibits leukocyte migration in vitro and in vivo. Proc Natl Acad Sci U S A. 2005; 102:14729–14734. [PubMed: 16203981]
53. Tadagavadi RK, Wang W, Ramesh G. Netrin-1 regulates Th1/Th2/Th17 cytokine production and inflammation through UNC5B receptor and protects kidney against ischemia-reperfusion injury. Journal of immunology. 2010; 185:3750–3758.
54. Ranganathan PV, Jayakumar C, Mohamed R, Dong Z, Ramesh G. Netrin-1 regulates the inflammatory response of neutrophils and macrophages, and suppresses ischemic acute kidney injury by inhibiting COX-2-mediated PGE2 production. Kidney international. 2013; 83:1087–1098. [PubMed: 23447066]
55. Khan JA, et al. Systemic human Netrin-1 gene delivery by adeno-associated virus type 8 alters leukocyte accumulation and atherogenesis in vivo. Gene Ther. 2010
56. Dominguez H, et al. Metabolic and vascular effects of tumor necrosis factor-alpha blockade with etanercept in obese patients with type 2 diabetes. Journal of vascular research. 2005; 42:517–525. [PubMed: 16155368]
57. Larsen CM, et al. Interleukin-1-receptor antagonist in type 2 diabetes mellitus. The New England journal of medicine. 2007; 356:1517–1526. [PubMed: 17429083]
58. Lin Y, et al. The hyperglycemia-induced inflammatory response in adipocytes: the role of reactive oxygen species. The Journal of biological chemistry. 2005; 280:4617–4626. [PubMed: 15536073]
59. Yeop Han C, et al. Differential effect of saturated and unsaturated free fatty acids on the generation of monocyte adhesion and chemotactic factors by adipocytes: dissociation of adipocyte hypertrophy from inflammation. Diabetes. 2010; 59:386–396. [PubMed: 19934003]
60. Bachman ES, et al. betaAR signaling required for diet-induced thermogenesis and obesity resistance. Science. 2002; 297:843–845. [PubMed: 12161655]
61. Konner AC, et al. Insulin action in AgRP-expressing neurons is required for suppression of hepatic glucose production. Cell Metab. 2007; 5:438–449. [PubMed: 17550779]

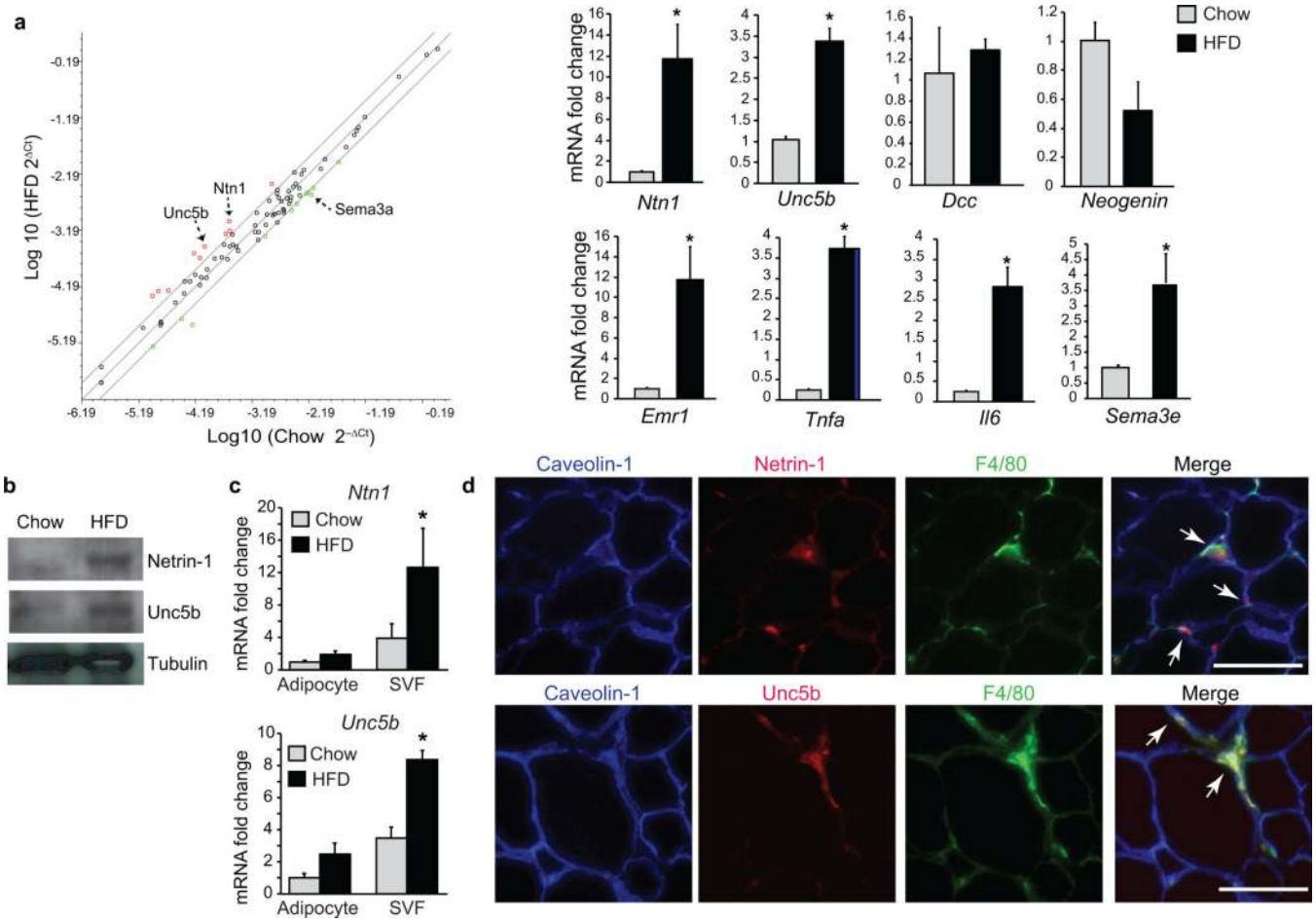

Figure 1. Netrin-1 and Unc5b are upregulated in obese-adipose tissue

(**a**) Scatter plot of neuronal guidance cue expression in VAT from mice fed a HFD or chow for 20 weeks: upregulated genes are indicated in red; downregulated genes in green ($n = 3$ mice/group). Confirmation of mRNA changes in VAT of mice fed chow ($n = 5$) or HFD ($n = 6$) by qRT-PCR (right panel). (**b**) Western blot of netrin-1, Unc5b, and tubulin in VAT from mice fed chow or HFD ($n = 3$). **(c)** Relative mRNA expression of *Ntn1* and *Unc5b* in the adipocyte and SVF fraction isolated from WAT of mice fed chow ($n = 4$) or HFD ($n = 6$). (**d**) Immunofluorescence staining for netrin-1 (red, upper) or Unc5b (red, lower), the macrophage marker F4/80 (green) and caveolin-1 (blue) in VAT of HFD-fed mice. Co-localization of netrin-1 or Unc5b with F4/80 is seen in yellow in the merged image (arrows). Scale bar = 100 μm. Data in a and c are the mean ± s.e.m. *$P < 0.05$.

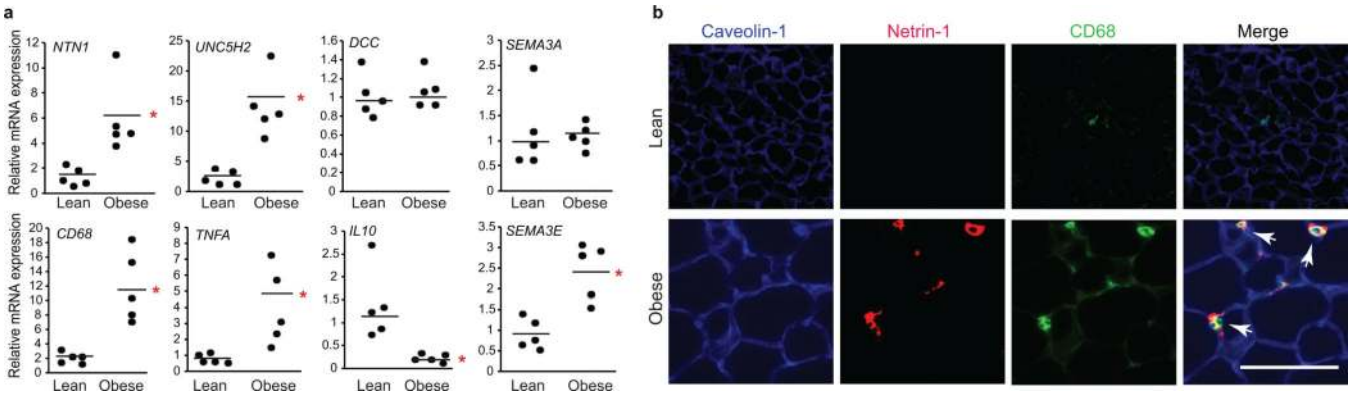

Figure 2. Netrin-1 is expressed by adipose tissue macrophages in obese human VAT

(**a**) qRT-PCR analysis of mRNA isolated from VAT of lean ($n = 5$) or obese ($n = 5$) human subjects. Data are the mean ± s.e.m. *$P < 0.05$. (**b**) Immunofluorescence staining of netrin-1 (red), caveolin-1 (blue), and CD68 (green) in VAT of lean and obese individuals. Co-localization of netrin-1 and CD68 is seen in yellow in the merged image (arrows). Scale bar = 100 μm.

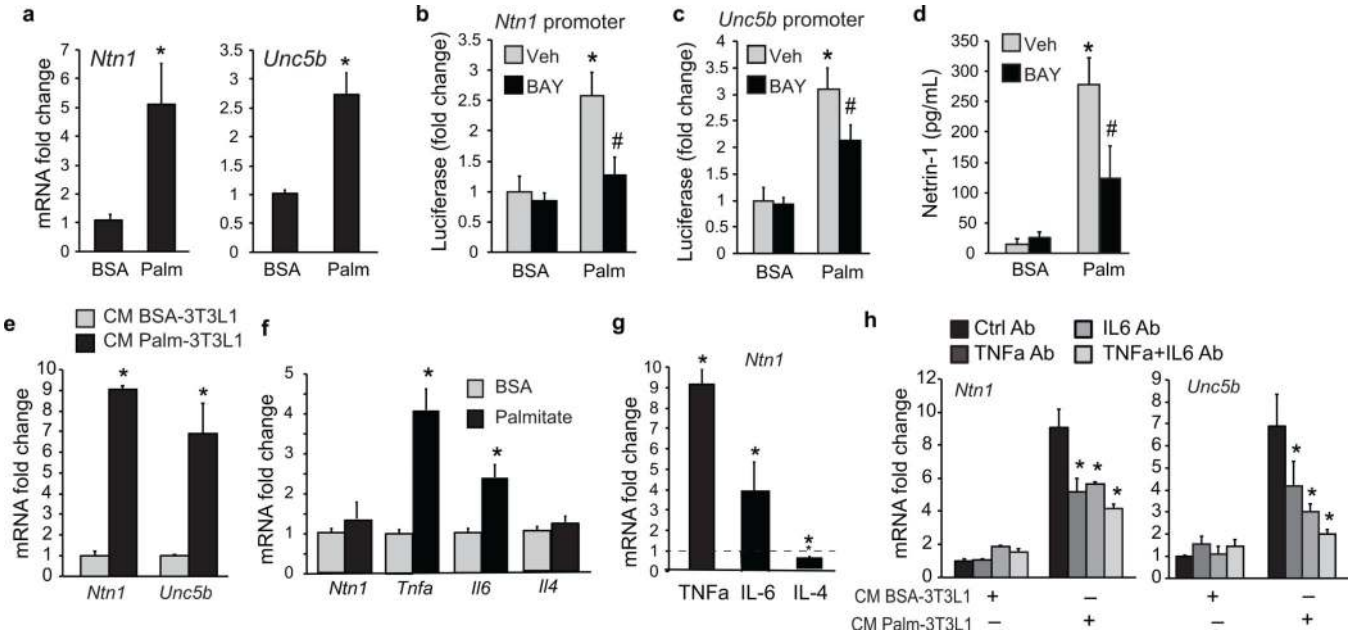

Figure 3. Palmitate upregulates *Ntn1* and *Unc5b* expression in macrophages

(**a**) *Ntn1* and *Unc5b* mRNA in BMDM treated with 250 μM BSA or palmitate for 24 h. (**b**) *Ntn1* and (**c**) *Unc5b* promoter-luciferase reporter activity in HEK293T cells treated with 250 μM BSA or palmitate in the presence of the NFkB inhibitor BAY11-7082 (10 μmol/L) or vehicle (veh). (**d**) Concentration of netrin-1 in culture supernatants of BMDM treated with 250 μM BSA or palmitate for 24 h in the presence of BAY11-7082 or vehicle. (**e**) *Ntn1* and *Unc5b* mRNA in BMDM treated with conditioned media (CM) from 3T3L1 adipocytes exposed to BSA or palmitate (250 μM) for 24 h. (**f**) qRT-PCR of mRNA from 3T3L1 adipocytes treated with BSA or palmitate (250μM) for 24 h. (**g**) *Ntn*1 mRNA in BMDM treated with TNFα (10 ng/ml), IL-6 (40 ng/ml) or IL-4 (10 ng/ml) for 24 h. (**h**) *Ntn1* and *Unc5b* mRNA in BMDM treated with CM from 3T3L1 adipocytes exposed to BSA or palmitate (250 μM) in the presence or absence of anti-TNFα, anti-IL-6 or both. Data presented are the mean ± s.d. of triplicate samples from a single experiment and are representative of three independent experiments. *$P < 0.05$.

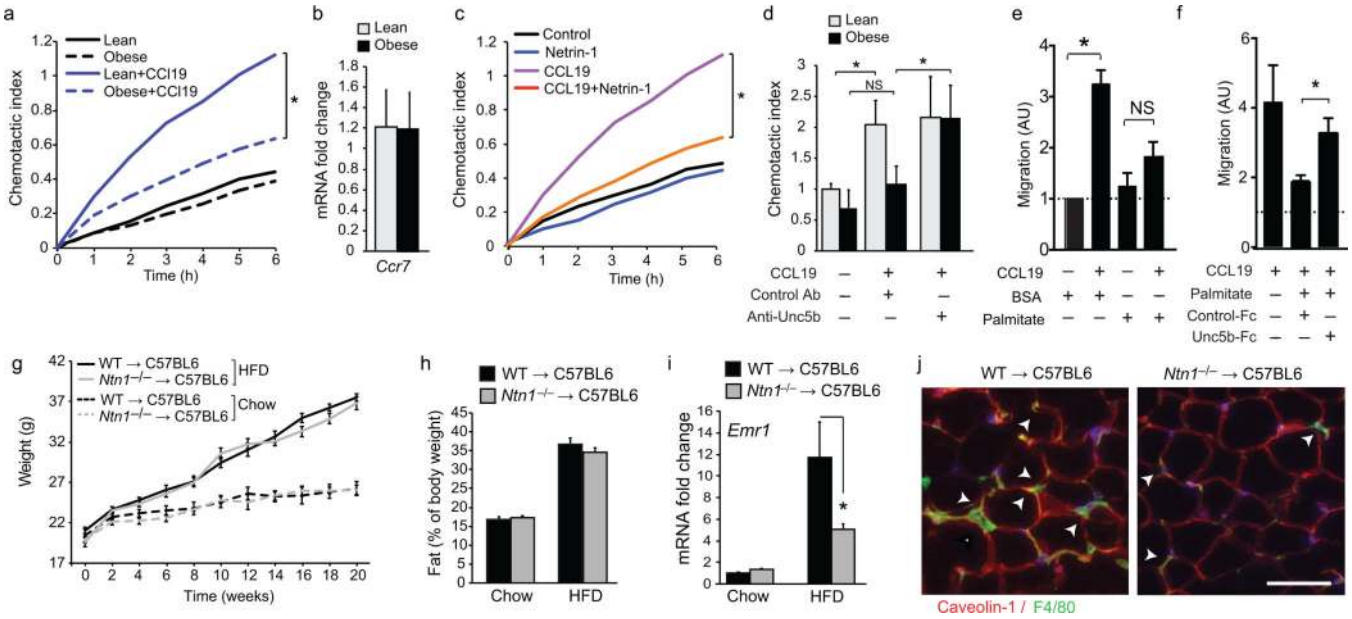

Figure 4. Netrin-1 blocks chemokine-induced migration of ATM and promotes ATM accumulation during HFD-feeding

(**a**) Real-time migration of ATM isolated from WAT of lean (chow-fed) or obese (HFD-fed) mice to CCL19 (500 ng/ml). (**b**) *Ccr7* mRNA in ATMs isolated from lean or obese WAT. (**c**) Migration of ATM isolated from lean mice to CCL19, netrin-1 (250 ng/ml) or both. (**d**) Migration of ATM isolated from WAT of lean or obese mice to CCL19 in the presence or absence of UNC5b blocking antibody or isotype matched control antibody (Control Ab). (**e–f**) Migration of peritoneal Mø pretreated with 250 μM BSA or palmitate toward CCL19 alone (e), or in the presence of Unc5b-Fc or isotype control (Control-Fc) antibody (f). (**g–h**) body weight (**g**) and fat mass **(h)** of C57BL6 mice transplanted with WT or *Ntn1*$^{-/-}$ bone marrow and fed chow (n = 7 per group) or HFD (n = 9 per group) for 20 weeks. (**i**) *Emr1* (F4/80) mRNA in VAT of mice of the indicated genotype fed a chow (n = 4) or western diet (n = 9). (**j**) Immunofluorescence staining for F4/80 in VAT of representative HFD-fed mice. Scale bar = 100 μm. Data in panels b,d-f are the mean ± s.d. of triplicate samples from a single experiment and are representative of three independent experiments. Data in g-i are the mean ± s.e.m. *P<0.05.

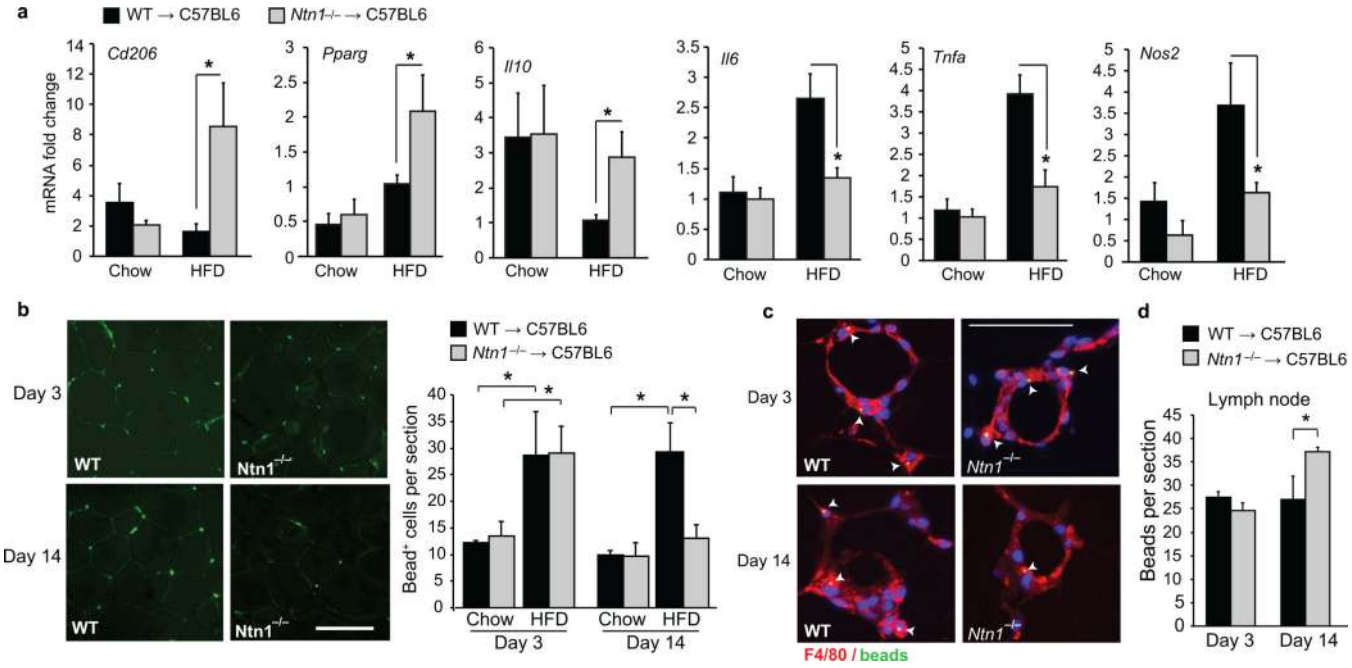

Figure 5. Netrin-1 promotes macrophage retention in adipose tissue during obesity

(**a**) qRT-PCR analysis of mRNA for M1 (*Nos2, Tnfa*, *Il6*) and M2 (*Cd206, IL10, Pparg*) markers in macrophages isolated from the VAT of mice fed chow ($n = 7$) or HFD ($n = 9$). **(b)** Analysis of macrophage recruitment and retention in VAT of mice fed a chow or HFD using a fluorescent bead-tracking model. Left: Representative images of fluorescent bead-labeled cells in VAT of HFD-fed mice at day 3 and 14. Scale bar = 100 μm. Right: Mean number of bead-labeled macrophages in VAT sections ($n = 5$ mice per group). (**c**) F4/80 staining (red) of VAT from HFD-fed mice 3 and 14 days post-labeling showing fluorescent beads (green) in macrophages in crown-like structures. **(d)** Mean number of beads in mesenteric lymph nodes on days 3 and 14 ($n = 5$ mice per group). Data in a, b, and d are the mean ± s.e.m. *$P<0.05$.

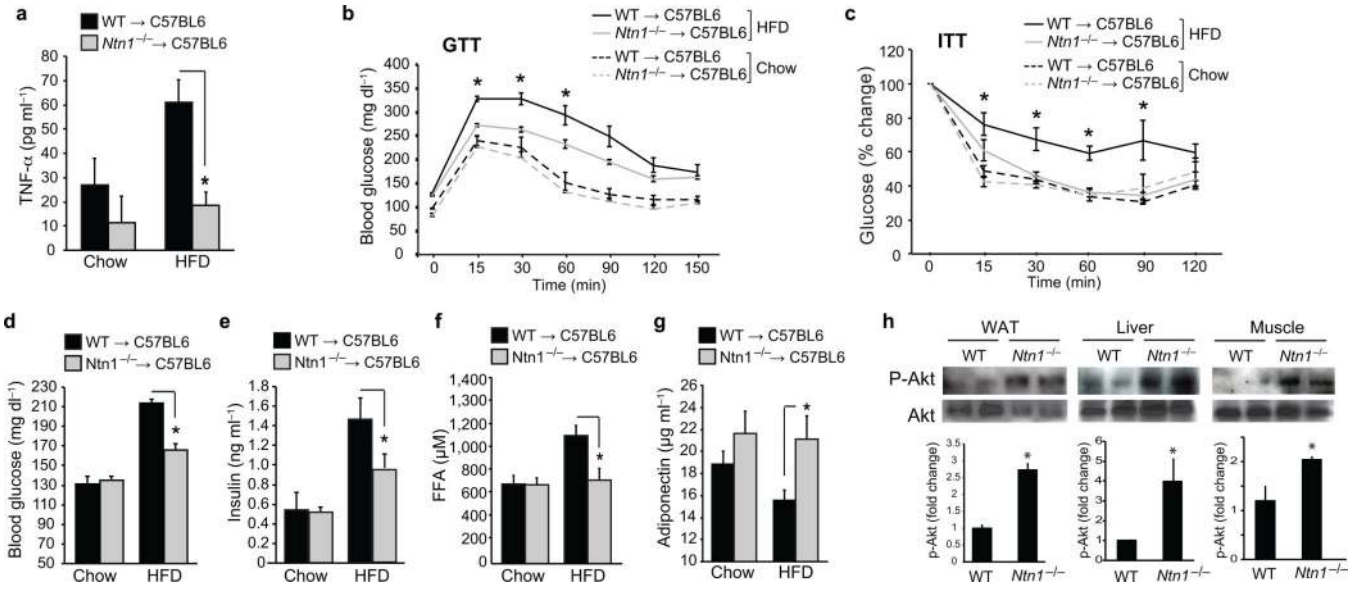

Figure 6. Netrin-1 expression by ATM promotes metabolic dysfunction

(**a**) Serum TNFα levels in mice transplanted with WT or *Ntn1*$^{-/-}$ bone marrow and fed chow (n = 5) or HFD (n = 6) for 20 wk. (**b**) Glucose tolerance test (GTT) and (**c**) Insulin tolerance test (ITT) of mice fed a chow (n = 7) or HFD (n = 9). (**d**) Blood glucose levels and plasma levels of (**e**) insulin, **(f)** free fatty acid (FFA), and (**g**) adiponectin of mice fed a chow (n = 7) or HFD (n = 9). **(h)** Western blot of phosphoAKT (Ser 473) and total AKT in white adipose tissue (WAT), liver and muscle. Quantification of p-Akt/total Akt is shown at bottom (n=4 mice/group). Data in a-g are the mean ± s.e.m. *P<0.05.